

## ELECTRICAL CONDUCTIVITY OBJECT LOCATOR: LOCATION OF SMALL METAL AND PLASTIC OBJECTS BURIED AT SHALLOW DEPTHS

D. C. Chin and R. Srinivasan  
Johns Hopkins University Applied Physics Laboratory  
Laurel, MD 20723-6099  
Telephone (301) 953-5000  
E-mail: daniel.chin@jhuapl.edu; vasan@aplcomm.jhuapl.edu

### INTRODUCTION

The electrical conductivity object locator (ECOL) technique maps conductivity values of the soil subsurface and characterizes buried foreign objects. The characterization includes location, size, and conductivity of foreign object. A typical example, also the objective of the work, is to locate small-sized plastic and metal objects buried in shallow depths. ECOL can also be used in the other physical bodies, such as concrete structures, composite materials, biological bodies, and other metallic and non-metallic structures to identify and characterize buried reinforcing bars (rebars), fibers, bullets, and fragments.

ECOL uses a low-amplitude ( $100\ \mu\text{A}$  –  $500\ \mu\text{A}$ ) electric AC current, single or multiple frequency. The impressed AC current generates AC potentials and magnetic fields throughout the site, which are measured at the surface and the boundary of the site. Also, ECOL establishes a finite element model to compute the surface and the boundary values of the site from the amount of current, the physical structure of the subsurface, and an assumed or a previous estimated conductivity profile of the subsurface. ECOL estimates the conductivity profile of the subsurface and the characters of the buried object by minimizing the sum of the square of the differences between the measured and the computed values. The minimization is based on a gradient approximation technique, namely, simultaneous perturbation stochastic approximation (SPSA). A finite element method (FEM) is used to compute the potentials or magnetic field along with the experimental

values (at the boundary) from a conductivity profile. The FEM process is called the “Forward Modeling”; the SPSA minimization is called the “Reconstruction” process.

In the field demonstration, the reconstruction procedure is used to locate a cylindrical object, a 20-cm-diameter and 5-cm-thick plastic or a 10-cm-diameter and 7-cm-thick metal, buried in a 3-m-wide by 1.5-m-deep soil region. The simulation studies used a block object, 20-cm-width, 10-cm-height, and 10-cm-thick. These objects are assumed to represent metal or plastic mines. ECOL uses an iterative process; the convergence of the ECOL takes place among 40 and 50 iterations in all cases. After 50 iterations, parameters reach near steady-state value. In the preliminary studies reported here, results are displayed after 100 iterations. Each iteration takes about 4-5 second of processing time on a 180 MHz Pentium.

The ECOL technique addresses a cluttered environment in which small- and large-sized items such as pebbles and plant roots may coexist with mines. Further, the ECOL technique assumes that the measured potential data likely *included* errors, and also is *contaminated* with electrical noise. It also makes no *a priori* assumption about the electrical conductivity of the soil or the buried objects. The technique *does* take into account the possibility of frequency-dependent variations in the conductivity (and dielectric constant) of the soil as well the buried objects. Hence, it employs current signals over a wide range of frequencies to get the best contrast in the

conductivity values. Unlike most other techniques, ECOL uses the SPSA algorithm, which tolerates a substantial amount of noise in the data and *does not* depend upon the accuracy of the measured potentials.

The heart of the reconstruction technique is the SPSA algorithm. It was presented in Spall (1988) and since refined in Spall (1992). The ruggedness and the applicability of the SPSA algorithm have been proved successfully on a wide variety of subjects ranging from traffic flow in inner cities (Spall and Chin, 1997) to automated quality control (Rezayat, 1995).

The ECOL technique has been verified using several simulated buried objects, both plastic and metal of various sizes, buried in soil of dimensions varying from a few meters to several hundred meters. Most importantly, the technique has been verified through this field experiment in which a metal or a plastic object size of a typical mine was buried in soil cluttered with pebbles and plant roots. The results of ECOL simulations and field demonstration are described in the following sections: Background, Methodology, Experimental, Finite Element Model, Reconstruction of the Internal Conductivity of the Mine Location, Simulation Studies, Field Demonstration Results, and Conclusion.

## BACKGROUND

Over the past 10 years, tools to locate buried objects have attracted attention from a wide variety of defense and civil industries (*Unexploded Ordnance Forum '97* and Ashley, 1996). Today, millions of objects, from small-sized land mines to large-size waste disposal and storage drums, remain buried worldwide. The task of reclaiming lands filled with mines, ammunition, and chemical wastes is far from simple. For this purpose, several types of specialized sensors are being developed to locate and characterize buried objects (Jet Propulsion Laboratory, 1995). Programs such as the

Strategic Environmental Research and Development Program (SERDP), sponsored by DoD and DoE, attempt to address questions related to the characterization and cleanup of such sites. Presentations at the *Unexploded Ordnance Forum '97* revealed that over the past decade there has been a worldwide effort to improve techniques for locating and characterizing the objects in subsurface. These techniques include electromagnetic and magnetometer sensors, ground penetrating radar, infrared, and several types of chemical and spectroscopic tools. Some progress has been made in performance enhancement of these techniques and in the miniaturizing the instruments, but there is room for improvement, specially in locating small-sized plastic and metal mines in cluttered soil subsurface.

At the Johns Hopkins University Applied Physics Laboratory (JHU/APL), we have initiated a new stochastic approach to locate small-size plastic and metal objects through characterization of soil subsurface conductivity. Subsurface conductivity measurements, sometimes termed conductivity-tomography or electrical-impedance-tomography, have been reported in the published literature since the late 1970s (Brown et al., 1994, Cook et al., 1994 and Smith et al., 1995). These measurements have been widely used in mapping the internal conductivity of biological bodies, as well as geological sites. These techniques involve placing electrodes around the sites with objects under investigation, and sending a known amount of electrical current through the site. The current generates electrical potentials or fields that are measured using another set of electrodes placed on that surface. Next, the internal conductivity of the object is reconstructed using the measured potential values, injected current, and the location of the electrodes. Several types of mathematical reconstruction algorithms have been used and reported since 1970s (Brown et al., 1994, Smith et al., 1995, and Wexler et al., 1985). Most of these techniques have attained a certain level of

qualified success: the subsurface conductivity can be mapped (1) when the differences between the conductivity values of the site elements and objects are small and (2) when the internal gradients of the potentials can accurately be calculated (Cook et al., 1994). However, none of these techniques has been successful in locating of plastic or metal mines buried at shallow depths.

In reality, objects buried under surfaces tend to have a wide range of electrical properties. Furthermore, accuracy in the potential measurements often cannot be assured. In addition, the current and potential data are likely to be corrupted with noise in the field, and measurement of distances between the locations of electrodes is also subject to uncertainties. The uncertainties in the data obtained under field conditions restrict the reconstruction of conductivity values using conventional gradient-based techniques (Brown et al., 1994, and Smith et al., 1995). For these reasons, locating small-sized objects such as mines through conductivity measurements has so far remained largely unsuccessful.

### Methodology

The ECOL technique maps and images the conductivity profiles of the subsurface at the region of interest by injecting electrical currents into the system. It is a noninvasive technique

that works in five major steps (see Figure 1). Steps 1 and 2 provide the experimental data needed for the reconstruction procedure described in Steps 3 - 5 that locates and characterizes the buried object.

- Step 1: Electrodes are placed around the site and connected to a power source. An electric current is injected into the site (Block 1 in Figure 1). The electric current generates electrical potentials in the entire site, including the surfaces.
- Step 2: The electrical potentials generated in Step 1 are measured using "reference electrodes" placed at the surface of the soil (Block 2 in Figure 1).
- Step 3: The subsurface of the site is divided into a large number of elements. Each element is given an initial arbitrary conductivity value (Block 3 in Figure 1).
- Step 4: This step consists of two subunits. Step 4a constructs a perturbation array from a random set of numbers generated from a Bernoulli distribution with outcome  $\pm 1$  and scaled by a step gain constant. The choice of the step gain constant is according to the requirements of SPSA. Then, it creates two perturbed conductivity profiles from adding and subtracting the perturbation array to and from a set of the previously estimated or assumed parameters (Block 4a in Figure 1). Step 4b computes voltage potentials for every element within the soil subsurface from the perturbed conductivity profiles using an FEM-bound algorithm (Block 4b in Figure 1).
- Step 5: The SPSA algorithm compares the two sets of computed boundary values from Step 4b with the measured values from Step 2 to approximate the gradients that update the parameters. If the termination criteria are not reached, the process returns to Step 4 for the next iteration (Block 5 in Figure 1).

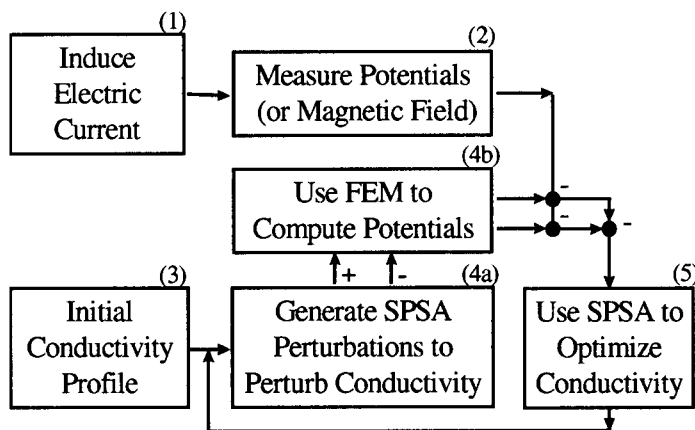
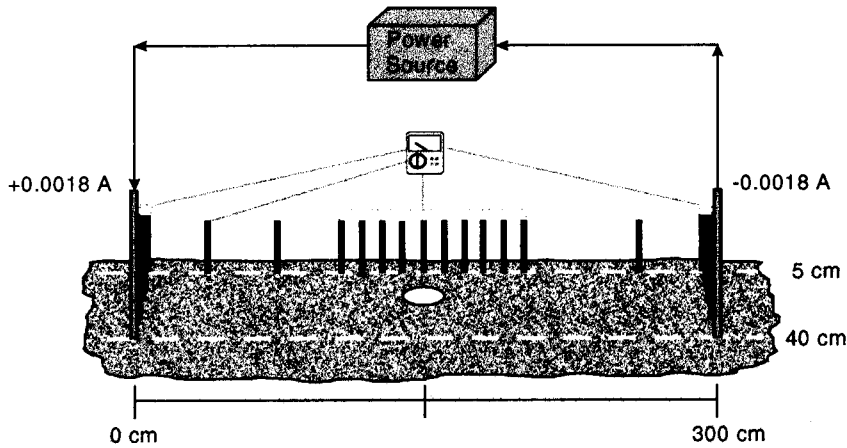


Figure 1: The Configuration of ECOL



**Figure 2: Diagram of the Demonstration Site**

In Figure 1, the “+” and “-” signs represent mathematical operations as they are described in the steps. In a simulation, the first two steps would be replaced by the boundary potentials computed from an assumed conductivity profile; the last three steps remain unchanged.

**EXPERIMENTAL**

The success of a technique can only be verified through experiments. Following the initial verification of the ECOL technique through simulated experiments, it was further validated through a field experiments. Figure 2 is a diagrammatic representation of the experimental site. A 20-cm-diameter and 5-cm-thick plastic object buried 20 cm below the surface is shown in the center of the diagram. This is the objective of our investigation. In the second

experiment, the plastic object was replaced by a 10-cm-diameter and 7-cm-thick metal object. The two outer ends of the diagram show two partially insulated metal rods inserted into the soil to a depth of 40 cm; the cylindrical surfaces of the rods were electrically insulated, leaving only the tips conducting. The rods were placed 300 cm from each other. The power source was a galvanostat capable of delivering constant current even under conditions of varying electrical resistance of the soil. A  $180 \pm 1 \mu\text{A}$ , low-frequency AC signal was

supplied through the summing junction of the galvanostat and forced into the ground through the two rods. The currents between the rods were regulated with the help of a silver/silver chloride reference electrode buried close to one of the two rods.

The flow of the AC current in the soil generated a set of electrical potentials throughout the volume of the soil between the two rods. Only the potential at the soil surface and along the boundary of the two rods were measured using silver/silver chloride electrodes and a spectrum analyzer. The locations of the silver/silver chloride electrodes are also shown in Figure 2; the distances between the electrodes and the rods were measured within an accuracy of  $\pm 1$  cm.

**FINITE ELEMENT MODEL**

The mathematical model of the experimental site used in FEM for computing the potentials is shown in Figure 3. It represents a cross section of the subsurface 100-m-deep by 500-cm-wide. The subsurface is divided into two sets of small divisions (rectangular blocks). Each division is called an element in FEM. The center region (50- by 90-cm) is the region of interest which consists of 45

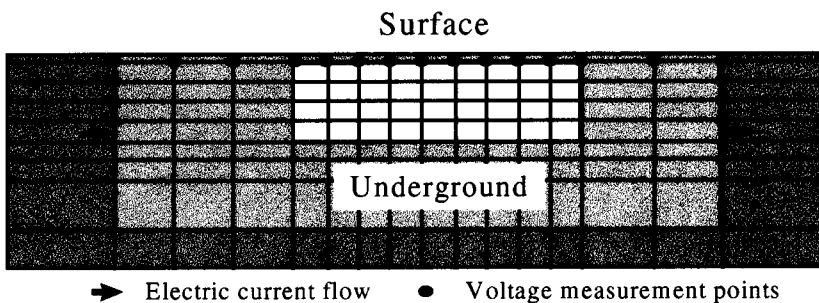


**Figure 3: Finite Element Model for Field Demonstration Site**

equal size rectangular elements. The gray shaded region located outside the center region is the region of influence which consists of 99 unequal size rectangular elements.

**RECONSTRUCTION OF THE INTERNAL CONDUCTIVITY OF THE MINE LOCATION**

The reconstruction process was described under Step 4a (SPSA) and Step 4b (FEM) in the Methodology section. A complete discussion of FEM can be found in *Finite Element Procedures in Engineering Analysis*. It solves the generalized Laplace equations mixed with Dirichlet and Neumann boundary conditions. This equation is called the Galerkin's error minimization method.

Step 3 through 5 (see Methodology) follow the SPSA algorithm. Note that ECOL follows two distinct parametric approaches, one (defined by Spall, 1992) for estimating the conductivity of the elements in the 50- by 90-cm middle section, and the other for the elements in the influence region outside the middle section. The conductivity of the elements in the later section are not optimized; they are kept at the same values throughout the iterations. The loss function mentioned in the SPSA algorithm for the ECOL technique is the sum square of the differences of the measurements vs. the (FEM) computed values. The gain sequence used in

SPSA is modified to avoid multiple solutions. The discussion of the global optimization algorithm can be found in Chin (1994).

**SIMULATION STUDIES**

In addition to the field experiments, two simulation studies are reported here. Both simulations use the field test setting and assumed the soil conductive value as  $10^{-3}$  to  $10^{-5} \Omega^{-1}m^{-1}$ . The purposes of the simulations was to test ECOL and to locate an object other than plastic.

The first simulation was conducted using a simulated buried plastic object. The object occupied two elements (the fifth and sixth blocks from the left on the second row on the map in figure 4); its conductivity value was  $10^{-8} \Omega^{-1}m^{-1}$ . Figure 4 also shows the reconstruction conductivity values in log scale only on the region of interest (i.e., the 50- by 90-cm middle region). The log conductivity for soil elements has values between -3 and -5 and the plastic elements have a value -8. The reconstructed conductivity value for the plastic (see table of figure 4) is larger than -8, because the estimated size of object did not occupy one whole element. The map and table indicate that there is a plastic object located between elements 4 and 6 of the second row.

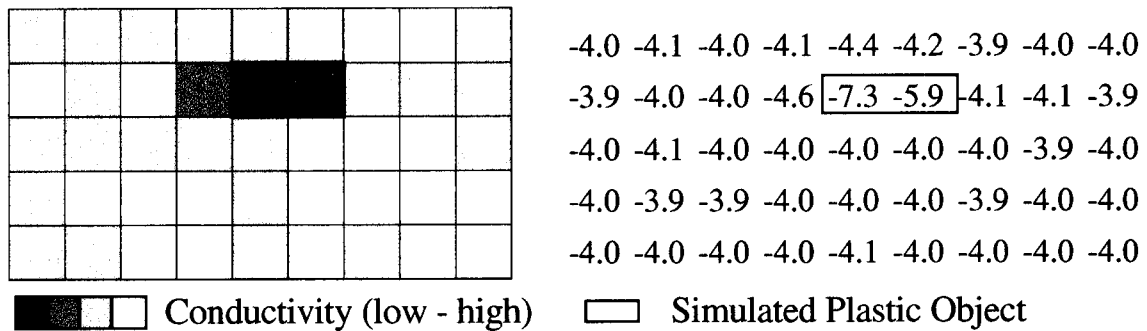


**Figure 4: Reconstruction of the Conductivity Profile for a Simulated Plastic Object**

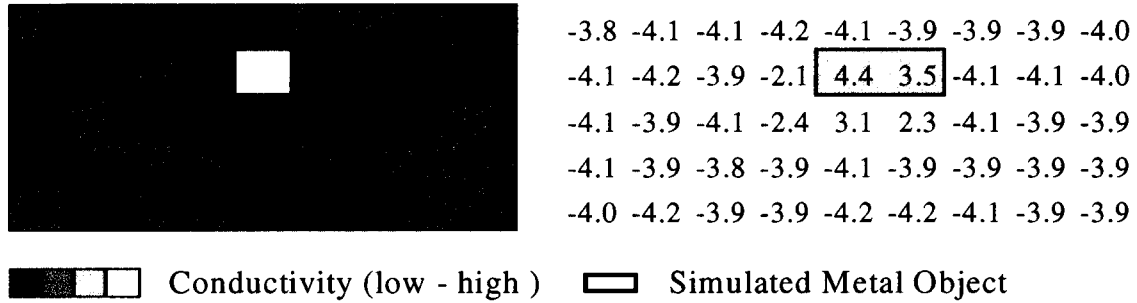


**Figure 5: Reconstruction of the Conductivity Profile for a Simulated Metal Object**

The second simulation study used a metal object. The conductivity of the metal was  $5.56 \times 10^4 \Omega^{-1}m^{-1}$ . Figure 5 shows the reconstruction results in log scale. The log conductivity for the metal object is 4.7. The reconstructed conductivity for metal is smaller than shown on the table, that is, the object occupies only a fractional part of elements.

**FIELD DEMONSTRATIONS**

The applicability of ECOL to locate mine-sized objects was demonstrated through two separated sets of field tests. In test 1, a 20-inch-diameter by 5-cm-thick plastic object was buried and located. Once immediately (30 minutes) after burial and next about 5 months after burial. In Test 2, a 10-cm-diameter by 7-cm-thick metal object was buried and located immediately (30 minutes) after burial. In both cases, the soil was not specially modified for test or demonstration purposes; the items, pebbles and the plants, present in the site were left mostly undisturbed. The test objects were buried only 10-15 cm

below the soil surface. The total area of the site tatat was tested uses approximately 300 cm by 300 cm the results of the tests are described below.

**TEST1: LOCATION OF PLASTIC SUBJECT**

Figure 6 shows the reconstructed subsurface conductivity for the field experiment with the buried plastic object. Only the middle section around the location of the object is shown. The plastic object is located between fourth and fifth elements from the left on the second row of the figure and occupied only parts of both elements. Note that the low-conducting plastic object is clearly visible in the table. The estimated location is 5 cm left of the buried site and is omitted form the figure. In addition, the conductivity of the soil, which is much higher than the object, is nonuniform. We attribute this to the presence of pebbles and roots in the soil. The numbers shown here emerged after only 100 iterations and took less than 5 minutes in a Pentium-equipped computer.

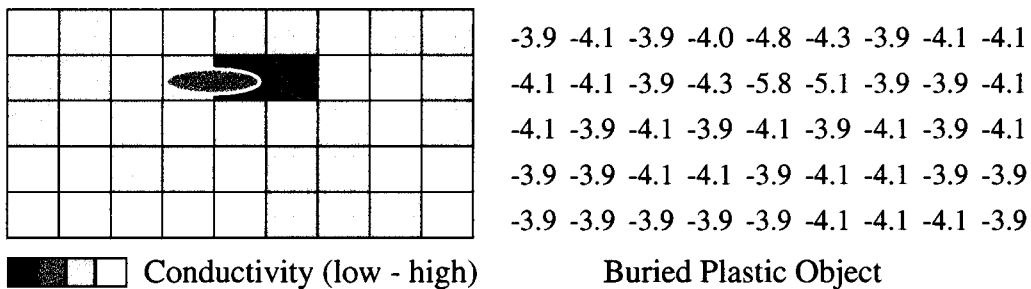


**Figure 6: Reconstruction of the Conductivity Profile for a Buried Plastic Object**

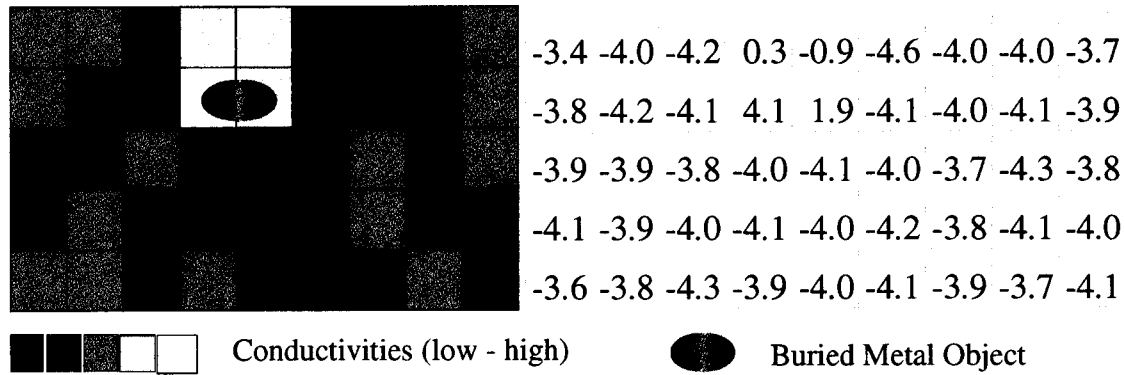


**Figure 7: Reconstruction of the Conductivity Profile for a Buried Metal Object**

Note that this experiment was conducted under a virtual blindfold condition, in which the algorithm made no *a priori* assumption about the size, location, or conductivity of the plastic object or the conductivity of the soil.

TEST2: LOCATION OF METAL OBJECT

Figure 7 shows the reconstructed subsurface conductivity for the field experiment with the buried metal object. Contrast from the plastic material, the metal object has higher conductivity than the soil conductivity. The higher estimated conductivity values indicate that these elements contain metal substances which are the fourth and fifth elements from the left on the first and second rows as they are shown in Figure 7. Although, the TEST 1 and TEST 2 were conducted at the same site, the soil condition were different. The estimated conductivity values for the elements with the soil substance are respectively different. Similar to the previous test, this test was also conducted under a virtual blindfold condition.

CONCLUSIONS

The purpose of the Electrical Conductivity Object Locator is to generate an internal map of the location, size, and conductivity of all objects inside the perimeter of a site suspected of having plastic and/or metal mines. In this work, we have demonstrated that the ECOL technique is

able to locate small-sized plastic and metal objects buried in shallow depths in cluttered soil.

The ECOL technique assumes spatial nonuniformity for conductivity of the soil subsurface. It divides the subsurface space into several elements, and assumes that the objects of interest are present within some of those elements. The technique injects a small-amplitude, low-frequency electrical current into the soil and measures the resulting electrical potentials at the soil surface. The conductivity of each element of the subsurface is reconstructed using the injected current as the input parameter and the measured potentials as the boundary condition. A sequence of algorithms, all of which were developed at the Johns Hopkins University Applied Physics Laboratory, is used in the reconstruction procedure. The heart of the procedure is the Simultaneous Perturbation Stochastic Algorithm (SPSA), which is quite *different* from other well-known conventional gradient techniques. While the conventional gradient techniques can and do reconstruct successfully when accurate gradient (potential) values are available, they fail when the gradient values are inaccurate or contaminated with noise. Under most field conditions, one should expect and be prepared to deal with measurement inaccuracies, as well as noise in the data. The success of the SPSA algorithm is attributed to its ability to reconstruct even under extreme conditions of noise and

inaccuracies in the input parameters and boundary conditions.

Yet another practical advantage of the ECOL technique is that the current can be injected into the soil from a location that is away from the area of interest or where the mines are supposed to be present. However, the technique is limited by the need to insert the electrodes into the soil for measuring the potential. We plan to overcome this limitation by measuring the localized magnetic field generated by the impressed current using magnetometers traversing above the soil surface.

#### ACKNOWLEDGEMENT

This work was supported by the JHU/APL Independent Research and Development Program, Environmental Thrust Area. Mr. P. R. Zarriello helped in field measurements.

#### REFERENCES

- [1] Proceedings of the conference *Unexploded Ordnance Forum '97*, 1997, Nashville, TN, May 28-30.
- [2] "Sensors Technology Assessment for Ordnance Explosive Waste Detection and Location," Jet Propulsion Laboratory, Cal. Inst. Tech., Pasadena, CA, 1995.
- [3] "Finite Element Procedures in Engineering Analysis," Eds.: K. Bathe, The Southeast Book Company, Prentice-Hall, Inc., New Jersey, 1982.
- [4] Ashley, S., 1996, "Search for Land Mines," *Mechanical Engineering*, pp. 62-67.
- [5] Brown, B. H., D. C. Barber, W. Wang, Liquin Lu, A. D. Leathard, R. H. Smallwood, A. R. Hampshire, R. Mackay, and K. Hatzigalanis, 1994, "Multi-Frequency Imaging and Modeling of Respiratory Related Electrical Impedance Changes," *Physiol. Meas.*, Vol. 15, A1-A12.
- [6] Brown, B. H., D. C. Barber, A. H. Morice, and A. D. Leathard, 1994, "Multi-Frequency Imaging and Modeling of Respiratory Related Electrical Impedance Changes," *IEEE Trans. Biomed. Eng.*, Vol. 41, No. 8, pp. 729-733.
- [7] Chin, D. C., 1994, "A More Efficient Global Optimization Algorithm Based on Styblinski and Tong," *Neural Networks*, Vol. 7, No. 2, pp. 573-574.
- [8] Cook, R. D., G. J. Saulnier, D. G. Gisser, J. C. Goble, J. C. Newell and D. Isaacson, 1994, "ACT3: A High-Speed, High-Precision Electrical Impedance Tomograph," *IEEE Trans. Biomed. Eng.*, Vol. 41, No. 8, pp. 713-722, and references therein.
- [9] Rezayat, F., 1995, "On the Use of an SPSA-based Model-free Controller in Quality Improvement," *Automatica*, Vol. 31, pp. 913-915.
- [10] Smith, R. W., I. L. Freeston, and B. H. Brown, 1995, "A Real-Time Electrical Impedance Tomography System for Clinical Use- Design and Preliminary Results," *IEEE Trans. Biomed. Eng.*, Vol. 42, No. 2, pp. 133-140, and references therein.
- [11] Spall, J. C., 1988, "A Stochastic Approximation Algorithm for Large-Dimensional System in the Kiefer-Wolfowitz Setting," *Proceedings of IEEE Conference in Decision Control*, pp. 1544-1548.
- [12] \_\_\_\_\_, 1992, "Multivariate Stochastic Approximation Using a Simultaneous Perturbation Gradient Approximation," *IEEE Transactions On Automatic Control*, v. 37, pp. 332-341.
- [13] Spall J. C. and D. C. Chin, 1997, "Traffic-Responsive Signal Timing for System-Wide Traffic Control," *Transportation Research Board 76<sup>th</sup> Annual Meeting*, 12-16 January 1997, Washington, DC, Paper No. 97-0454.
- [14] Wexler, A., B. Fry and M. R. Neuman, 1985, "Impedance-Computed Tomography Algorithm and System," *Applied Optics*, Vol. 24, No. 23, pp. 3985-3993.